The Journal of the Oceanological Society of Korea
Vol. 21, No. 3, p. 171-183, September 1986.

Variation of the M2 tide amplitude around the Jeju-Do

Kuh Kim and Sang Ho Lee
Department of Oceanography, Seoul National University

제주도 주변 M2조의 진폭 변화

김 구 · 이상호
서울대학교 해양학과

Abstract

The amplitudes of the M2 tide recorded at Seoguipo and Jeju are 77.9 cm and 70.1 cm respectively, which differ by 7.8 cm over a distance of 30 km across the Jeju-Do. The difference is an example of the geographical variation of the tidal amplitude around the Jeju-Do, the larger amplitude being along its southern coast compared with that along its northern coast. This variation can be explained in terms of effects of an island on the wave propagation as modelled by Proudman (1914). A numerical experiment of the M2 tide around the Jeju-Do reproduces the basic pattern of the observed variation and results are consistent with the theory. Due to the rotation of the earth larger and smaller amplitudes result along the left-hand and right-hand coasts of an island for an observer facing the direction of the wave propagation in the northern hemisphere.

요약 : 서귀포와 제주항에서 기록된 M2조의 진폭은 각각 77.9 cm와 70.1 cm로서 7.8 cm의 차이가 제주도를 가로지르는 30 km의 거리에서 일어난다. 이러한 차이는 진폭이 제주도의 남쪽 해안에서는 크고, 북쪽 해안에서는 작은 지역적 변화의 한 예이다. Proudman (1914)의 이론과 같이 평면파의 전파가 섬에 의하여 산란되는 효과로서 위의 현상은 설명될 수 있다.

수치실험은 자료가 보여주는 진폭의 변화상을 재현하였고, 이론과 일치하는 결과를 보였다. 지구 자전의 효과로 인하여 조석파가 진행하는 방향을 바라보며 섬의 왼쪽에 위치한 해안에서는 큰 진폭이, 그리고 오른쪽에 위치한 해안에서는 상대적으로 작은 진폭이 나타나게 된다.

INTRODUCTION

Propagation of tidal waves around the Jeju-Do (Island) produces interesting sea level variations along its coast. Ogura (1933) shows that the M2 tide propagates progressively from the southeast to the northwest around the Jeju-Do and Choi (1980) reproduced the same pattern in a numerical model. Fig. 1 shows that the amplitudes of the M2 tide measured at seven locations differ quite significantly with a range of 61.2-77.4 cm. It can be noticed that the variation of amplitude depends upon the geographical location of tidal measurements. At two sites on the southern side of the island the amplitude appears with the large magnitudes of 77.0 cm and 77.4 cm. On the other hand the lowest amplitude, 61.2 cm, is recorded at the northeastern corner of the island and the amplitudes are relatively small along this part of the coast. In consistence with this geographical pattern, ranges of the spring tide are 261 cm at Seoguipo and 243 cm at Jeju, and those of the neap tide are 194 cm and 183 cm respectively (Hydrographic Office, 1982).

Since most of the M2 amplitudes and the spring and neap tides are estimated based

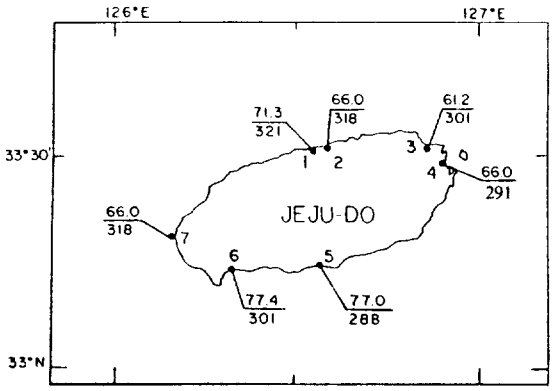

Fig. 1. Variation of the M2 tide around the Jeju-Do. Upper and lower numbers are amplitude in cm and phase in degree refered to 135°E measured at Jeju(1), Whabukri(2), Sewha(3), Udo(4), Seoguipo(5), Whasun(6), and Chagui-Do(7). Data are from Choi(1980).

upon relatively short tidal records of less than one month, it is obvious that longer records are needed to ensure the estimates. At present, long-term data are available only at Jeju and Seoguipo, where measurements started 1964 and 1985 respectively. We have analyzed the six-month data from these stations and results are summarized in Table 1. Encouragingly enough, the M2 amplitudes at Jeju and Seoguipo in Table 1 are nearly the same as shown in Fig 1. It is important to note in Table 1 that other main tidal constituents also record larger amplitudes at Seoguipo than at Jeju by 10% or more, implying that the differential variation is not limited to the M2 tide. Details of our analysis will be published separately later.

Table 1. Tidal constants at Jeju and Seoguipo calculated from the sea level data taken during January–June 1985 (phase referred to 135°E).

		Jeju		Seoguipo	
Component	Period (hour)	Amplitude (cm)	Phase (degree)	Amplitude (cm)	Phase (degree)
O1	25.819	16.3	199.1	17.5	189.2
K1	23.934	21.9	219.2	23.9	208.4
N2	12.658	15.7	299.5	17.2	283.6
M2	12.421	70.1	315.1	77.9	291.4
S2	12.000	29.4	347.9	35.0	319.2
MK2	11.967	7.9	333.7	10.1	309.2

As another means to supplement the short records we also examine results of the numerical model by Choi (1980), who showed that the M2 amplitude increases towards the southern coast of the Korean Peninsula as a general trend in the area (Choi, 1980; Fig. 6). However, Choi (1980) made no specific attempt to understand the detailed, regional variation around the Jeju-Do. We construct a co-tidal chart for seas around Jeju-Do based upon the data from the model by Choi (1980). In Fig. 2 the amplitude of the M2 tide along the southern coast of the Jeju-Do is consistently larger than that along the northern coast. It should be noticed, however, that numerical results of the M2 amplitude around the Jeju-Do are in general substantially larger than the observed values shown in Fig. 1, although the model simulated general features of tides in the Yellow Sea and the East China Sea. It is of importance that the difference between the amplitudes along the southern and northern coasts of the Jeju-Do is opposite to the general trend of the increasing amplitude towards the southern coast of Korean Peninsula from the East China Sea. This contrast makes one suspect that the observed variation of the M2 amplitude around the Jeju-Do might be an effect of the island on the propagation of the tidal wave.

Kang (1984) made an analytic model of the M2 tide near the Jeju-Do in terms of incident and scattered waves. According to this analytic model an amplification of the tide occurs along the northeastern coast and a reduction along the southwestern coast, the results being inconsistent with the observations. Kang (1984) vaguely attributes this discrepancy to the deviation of the model geometry from the island coast, non-uniform topography and the scattering effect by the southern coast of the Korean Peninsula. However, it does not seem that any of these would affect the wave propagation so drastically to explain the observed variation. The coast of the Jeju-Do is shaped

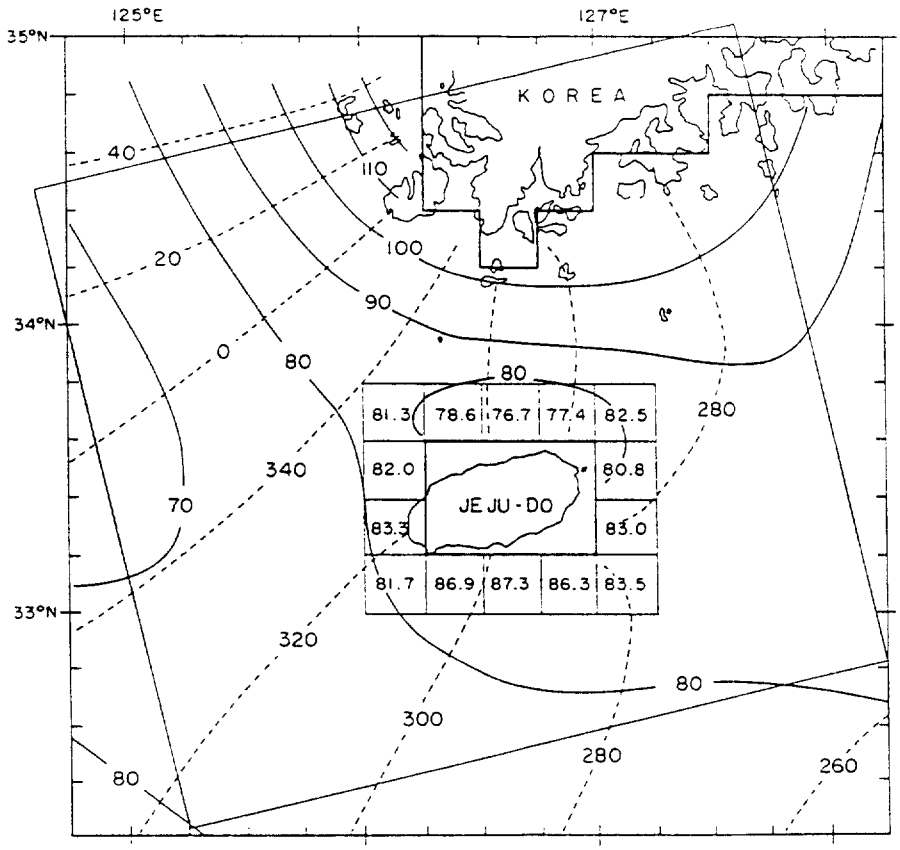

Fig. 2. Co-tidal chart based upon results of numerical experiment by Choi (1980). Solid and dotted lines indicate amplitudes in cm and phases in degree refered to 135°E. Numbers in squares around the Jeju-Do are the amplitudes at grid points near the Jeju-Do. The tilted boundary indicates the boundary for numerical experiments in this study.

very close to an ellipse as approximated by Kang (1984), the Jeju-Do rises very sharply from a nearly flat bottom, and the southern coast of the Korean Peninsula should not affect the wave propagation near the Jeju-Do as much as the Jeju-Do does.

This paper concerns the dynamical cause for the variation of the M2 tide around the Jeju-Do which is yet to be understood. We briefly examine the theoretical work by Proudman (1914), who first investigated the effect of an island on the propagation of a plane wave. Then numerical models are constructed for two kinds of incident waves; one for a plane weve and the other for the M2 tide with the open boundary condition adopted from Choi (1980). Theory, numerical experiments and observation are compared each other in details.

THEORY

For a rotating water of uniform depth with a constant angular velocity ω, Proudman (1914) considered the diffractions of a plane wave by objects whose linear dimensions are small compared with a wavelength, near the objects themselves. For our study it is worthwhile to examine the solution for the case of an elliptic island. According to Proudman (1914) the elevation of a free surface is given by

$$\zeta = \{1 - \frac{2\omega\sigma\kappa Ce^{2a-\xi}}{\sigma^2 - 4\omega^2}(l\sin\eta - m\cos\eta)\}$$
$$\cos(\sigma t - \epsilon) \qquad (2.1)$$

where

$$\epsilon = -\frac{\kappa Ce^{a}}{\sigma^2 - 4\omega^2}\{\sigma^2\cosh(\xi - a) - 4\omega^2\sinh$$
$$(\xi - a)\}(l\cos\eta + m\sin\eta) \qquad (2.2)$$

for the primary wave described by

$$\zeta_p = \cos\{\kappa(lx + my) + \sigma t\}, \qquad (2.3)$$

where the dispersion relationship is given by $\kappa^2 = (\sigma^2 - 4\omega^2)/gh$ and $l^2 + m^2 = 1, \sigma \neq 0$ and $\sigma \neq 2\omega$. Here the cartesian coordinates (x,y) are related to elliptic coordinates as follows

$$x = C\cosh\xi\cos\eta, \quad y = C\sinh\xi\sin\eta$$

where C is a focus distance and the shore of the island is given by $\xi = a$.

To delineate the effect of the scattering we can rewrite Eq. (2.1) as

$$\zeta = (1 + A)\cos(\sigma t - \epsilon), \qquad (2.4)$$

where A is the amplitude of the scattered wave, given by

$$A = S(\xi)\sin(\eta - \alpha). \qquad (2.5)$$

$S(\xi)$ represents the part which varies with ξ only and α specifies the propagation direction of the primary wave such that

$$S(\xi) = \frac{2\omega\sigma\kappa C}{\sigma^2 - 4\omega^2}e^{2a-\xi} \qquad (2.6)$$

and $l = -\cos\alpha$, $m = -\sin\alpha$. (2.7)

The amplitude of the scattered wave is expressed in Eq. (2.5) as a multiplication of two separate effects; one which varies with the distance from the island and the other which depends solely upon the angle with respect to the propagation of the primary wave. To illustrate the effect of the scattering we construct an amplitude-phase diagram (Fig. 3), which defines the theoretical relationship between amplitude and phase along the circumference ot the Jeju-Do. The diagram is for the following parameters which are chosen to compare the theory with numerical experiments later in this paper. In our case 2ω is equal to the Coriolis parameter at 33°20'N, σ the frequency of the M2 tide. The wavenumber κ is determined by the dispersion relationship for the water depth of 75m, and C and a are taken from Kang (1984) who approximated the Jeju-Do as an ellipse.

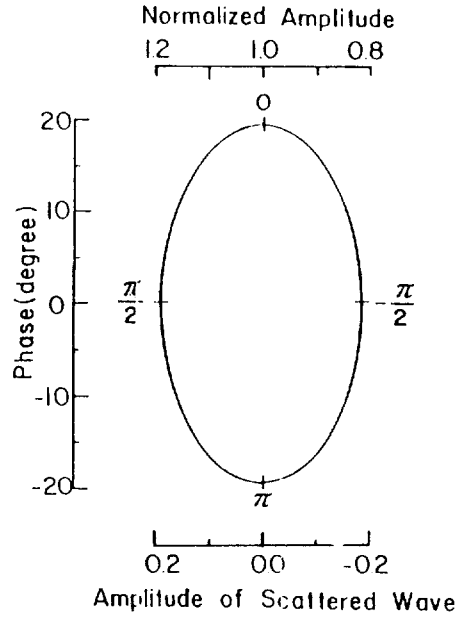

Fig. 3. Theoretical amplitude-phase diagram for the M2 tide around the circumference of the Jeju-Do. Upper and lower axis are the normalized total amplitude and that of the scattered wave. Amplitude is the same as that of the incident wave at $\eta - \alpha = \pi$ and $\eta - \alpha = 0$ which are the arrival and departure points of the tidal wave. Maximum and minimum of the tidal amplitude occur at $\eta - \alpha = \pi/2$ and $-\pi/2$ respectively.

$$2\omega = 0.8025 \times 10^{-4}\,\mathrm{sec}^{-1}$$
$$\sigma = 1.4051 \times 10^{-4}\,\mathrm{sec}^{-1}$$
$$\kappa = 4.252 \times 10^{-8}\,\mathrm{cm}^{-1}$$

$C = 3.12 \times 10^6$ cm
$a = 0.524$

Making use of Eqs. (2. 2) and (2. 5) it can be easily shown that the closed contour in Fig. 3 is an ellipse. From the phase it is noticed that the arrival and the departure points of the wave at the shore are $\eta = \alpha + \pi$ and $\eta = \alpha$, and the amplitude at these points is the same as that of the primary wave. The two particular points divide the circumference into two parts. Along one half where $0 < \eta - \alpha < \pi$ the amplitude is larger than that of the primary wave. Along the other half where $0 > \eta - \alpha > -\pi$ it is smaller than that of the primary wave. The amplitude reaches its maximum at $\eta - \alpha = \pi/2$ and its minimum at $\eta - \alpha = -\pi/2$. The magnitude of the amplitude of the scattered wave relative to that of the primary wave is 0.19 in case of the Jeju-Do. It is most interesting that the amplitude-phase diagram is antisymmetrical with respect to the wave propagation as far as the amplitude of the scattered wave, A, is concerned, as it varies with the sine function of the angle measured from the direction of the wave propagation in Eq. (2. 5). The antisymmetry is also apparent in case of the diffraction of a plane wave by a circular island (Proudman. 1914; Eq. 16).

NUMERICAL MODEL

The vertically averaged equations of continuity and motion in the sea of constant density, incorporating a quadratic bottom friction, take the following forms.

$$\frac{\partial \zeta}{\partial t} + \frac{\partial}{\partial x}(Hu) + \frac{\partial}{\partial y}(Hv) = 0 \tag{3. 1}$$

$$\frac{\partial u}{\partial t} + u\frac{\partial u}{\partial x} + v\frac{\partial u}{\partial y} - fv + \frac{ku(u^2+v^2)^{1/2}}{H} + g\frac{\partial \zeta}{\partial x} = 0 \tag{3. 2}$$

$$\frac{\partial v}{\partial t} + u\frac{\partial v}{\partial x} + v\frac{\partial v}{\partial y} + fu + \frac{kv(u^2+v^2)^{1/2}}{H} + g\frac{\partial \zeta}{\partial y} = 0 \tag{3. 3}$$

where the notations are

x, y	:	horizontal cartesian co-ordinates,
t	:	time,
ξ	:	elevation of the sea surface,
h	:	undisturbed depth of water,
H	:	total depth of water ($h + \xi$),
f	:	Coriolis parameter,
k	:	coefficient of bottom friction,
g	:	acceleration due to the earth's gravity,
u', v'	:	components of current in x and y, respectively,
u, v	:	components of the depth-averaged current given by

$$u = \frac{1}{H}\int_{-h}^{\zeta} u'dz, \quad v = \frac{1}{H}\int_{-h}^{\zeta} v'dz$$

The Eq. (3. 1), (3. 2) and (3. 3) are written into finite difference forms, following Flather and Heaps (1975), excluding the advective acceleration terms for simplicity, and using a spatial grid notation as shown in Fig. 4.

$$\frac{\zeta_i(t+\Delta t) - \zeta_i(t)}{\Delta t} = -\frac{1}{\Delta S}\{d_i(t)u_i(t) - d_{i-1}(t)u_{i-1}(t) + e_{i-n}(t)v_{i-n}(t) - e_i(t)v_i(t)\} \tag{3. 4}$$

$$\frac{u_i(t+\Delta t) - u_i(t)}{\Delta t} = fr_i(t) - g\frac{\{\zeta_{i+1}(t+\Delta t) - \zeta_i(t+\Delta t)\}}{\Delta S} - \frac{ku_i(t+\Delta t)\{u_i^2(t) + r_i^2(t)\}^{1/2}}{d_i(t)} \tag{3. 5}$$

$$\frac{v_i(t+\Delta t)-v_i(t)}{\Delta t} = -fs_i(t+\Delta t) - g\frac{\{\zeta_i(t+\Delta t)-\zeta_{i+n}(t+\Delta t)\}}{\Delta S} - \frac{kv_i(t+\Delta t)\{s_i^2(t)+v_i^2(t)\}^{1/2}}{e_i(t)} \quad (3.6)$$

where

$$\Delta S=\Delta x=\Delta y$$

$$d_i=\frac{1}{2}(H_i+H_{i+1}),\quad e_i=\frac{1}{2}(H_i+H_{i+n})$$

$$r_i=\frac{1}{4}(v_{i-n}+v_{i-n+1}+v_i+v_{i+1})$$

$$s_i=\frac{1}{4}(u_{i-1}+u_i+u_{i+n-1}+u_{i+n})$$

In order to solve these equations we need both initial conditions and boundary conditions. The calculation is started from a state of rest $\xi = u = v = O$, at $t = O$. At land boundaries the component of current normal to the boundary is set to zero. Along the open boundary of model the elevation is specified as

$$\zeta(t) = Z\cos(\sigma t - G)$$

where Z is the amplitude and G the phase. Then the component of current across the open boundary is calculated using the continuity equation. At a convex corner of the open boundary, each component of current is extrapolated based on Taylor series expansions from the known interior values following Flather and Heaps (1975).

The finte difference grid used for the model with bathymetry is shown in Fig. 5. The grid size is 5 km and the array has 51 × 58 elements. The x-direction of the model is tilted 14 degrees counterclockwise from the east in order to resolve the shape of the Jeju-Do well. The Coriolis parameter and the bottom frictional coefficient are taken to be constant as $f = 8.025 \times 10^{-5}$ sec^{-1} and $k = 0.0026$, respectively.

In all numerical experiments the period of incident waves is set to 12 lunar hours to simulate the propagation of the M2 tide. For the first experiment the depth is assumed constant at 75 m and an incident wave is directed to 154 degrees measured counterclockwise from the east. Along the open boundary a constant amplitude of 100 cm is assumed and the phase is specified according to the propagation of a shallow water wave in a rotating frame. For the second experiment a realistic topography as shown in Fig. 5 with the maximum depth of 122 m is introduced, and the amplitude and phase along the open boundary are adopted from the model of the M2 tide in the Yellow Sea and the East China Sea by Choi (1980). In all experiments the time-step of 1/40 of one lunar hour is chosen to satisfy the explicit stability condition and steady states are achieved after 10 lunar periods. Differences in the elevation and the velocity of the 11th period run at several test grid points compared with the 10th period run are less than 0.1 cm and 0.1 cm/sec respectively. Fol-

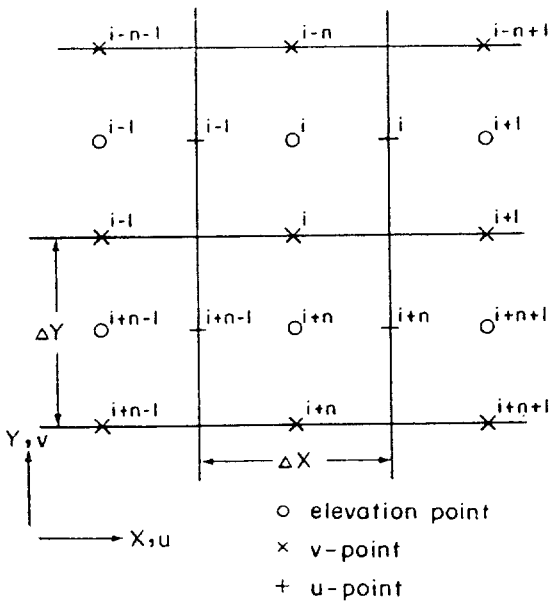

Fig. 4. Grid scheme for numerical experiments.

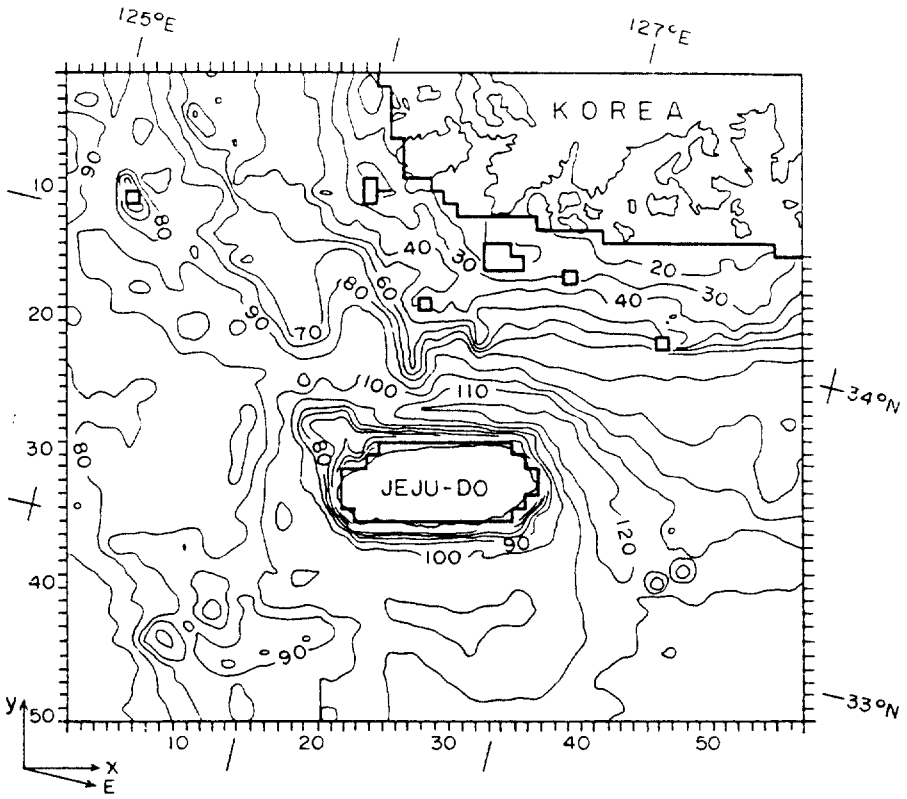

Fig. 5. The finite difference grid of the sea around the Jeju-Do with bathymetry (depth in meter). Domain is tilted 14° counterclockwise from the east to resolve the Jeju-Do well.

lowing results are obtained by the Fourier analysis of the 11th period run.

MODEL RESULTS

A Plane Wave

The distribution of the phase and amplitude of the M2-period wave is presented in Fig. 6a and b. Away from the Jeju-Do the phase lines are nearly parallel to each other in accordance with the propagation of the plane wave specified along the open boundary. Near the Jeju-Do, particularly around the northeastern and southwestern shores of the island, the phase lines are bent to conform to the curved coastline. Upon the arrival of the wave on the southeastern shore of the Jeju-Do it propagates separately along the northern and the southern coasts, and merges on the other side of the island after the completion of its propagation around the island.

Fig. 6b shows the deviation of amplitude from the incident wave, which is very useful to examine the effect of the Jeju-Do. It is easily noticed that the effect of the island is limited around the Jeju-Do, extending about the distance of the size of the Jeju-Do from its shore. The effect appears as a pair of positive and negative deviations off the southern and northern coasts. The shore of the Jeju-Do is also divided into two parts associated with the deviation. Extreme positive and negative deviations occur at the southwestern and northeastern shores. This pattern of the amplitude and phase variation is consistent with the theoretical amplitude-phase diagram shown in Fig. 3. It is also worthwhile to compare the

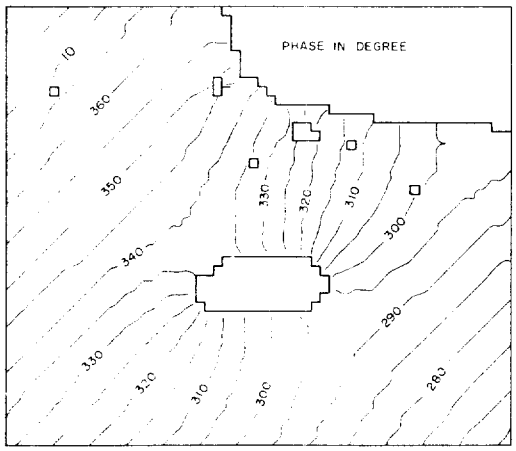

(a)

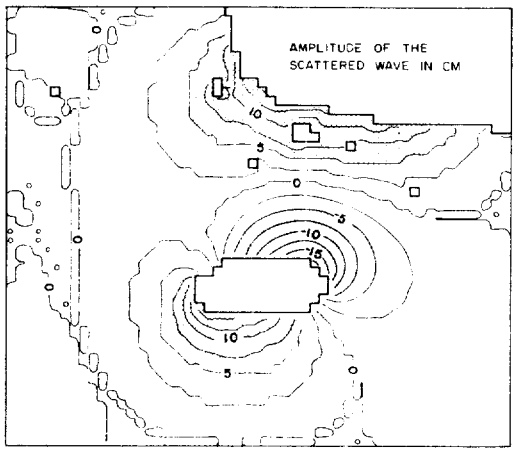

(b)

Fig. 6. Phase(a) and amplitude(b) distribution for the plane, incident wave. Positive and negative deviations of the amplitude from the incident wave with magnitudes greater than 5 cm are dotted and shaded for convenience.

results of the numerical model with the theory quantitatively. It is noticed that the extreme deviations of 17.0 cm and -18.5 cm are nearly of the same magnitude in agreement with the theory. Furthermore, the deviations are very close to the theoretical estimate based upon Eq. (2. 6). As can be seen in Fig. 3 the magnitude of the scattered wave amplitude for the parameters given in Theory is 19.0 cm, which is compared very favorably with the numerical results.

The good agreement between theory and the numerical experiment deserves more dynamical explanations for the differential variation of the amplitude. As pointed out by Pedlosky (1979, p74), the plane wave is not in geostrophic balance and the current vector of the wave traces an ellipse, as can be seen in Fig. 7, away from the Jeju-Do. However, near the island, particularly along the coastline, the current is parallel to the coast and rectilinear due to the boundary condition. As the cross-shore component of the current vector is negligibly small, the Coriolis force due to the long-shore component of the current vector in the cross-shore component of the momentum equations (Eq. 3. 3) is balanced by the pressure gradient force except for the friction. This dynamics are very similar to the case of the well-known Kelvin wave, in which the geostrophic balance produces a sloping sea surface. During a flooding period current flows in the direction of the wave propagation and the sea level rises to its right. For an observer facing the direction of the wave propagation, this produces a higher and lower sea level on the left-hand and the right-hand coasts of the island as shown in Fig. 8. On the other hand, during an ebbing period the current reverses

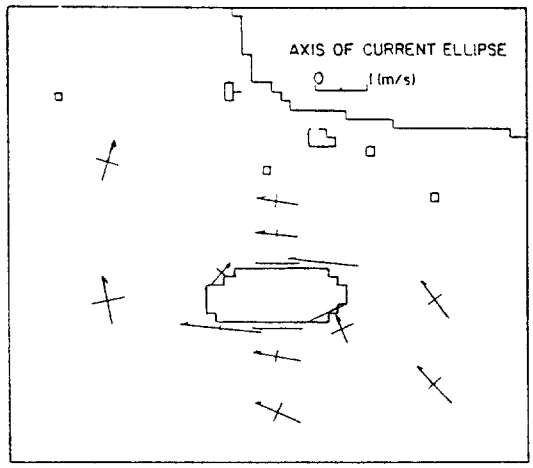

Fig. 7. Major and minor axis of current ellipse. Arrows indicate clockwise rotation of current vectors.

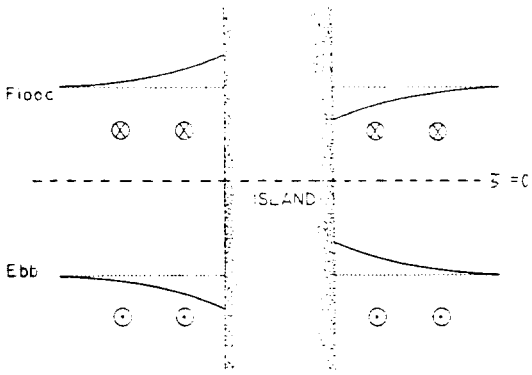

Fig. 8. Schematic cross section of the sea level at high and low tides. Conventional notations are used for the direction of currents. Dotted lines are the sea levels without the rotation of the earth.

its direction, opposite to the direction of the wave propagation, and for the same observer as during the flooding period the geostrophic balance produces a lower and higher sea level on the left and the right of the island. As the net effect of this temporal change the amplitude is larger and smaller on the left-hand and the right-hand coast of an island, facing the direction of the wave propagation, which happens to be the southwestern and northeastern coast of the Jeju-Do. Obviously this differential variation is not possible without the rotation.

It is also noticed in Fig. 6b that the amplitude increases toward the southern coast of the Korean Paninsula. Since the amplitude along the open boundary is fixed at 100 cm, the amplitude tapers towards the eastern and northern ends of the southern coast. Due to this tapering the variation of the amplitude along the southern coast with a maximum deviation of about 15 cm looks rather similar to that around the southwestern shore of the Jeju-Do. It seems to be clear that the larger amplitudes on the southern coasts of the Jeju-Do and of the Korean Peninsula are of same dynamical origin as illustrated in Fig. 8.

The M2 Tide

The purpose of this experiment is to examine the detailed variation of the M2 tide around the Jeju-Do. Since there are no tidal or current data observed in the open sea for the use of specifying the open boundary condition, we rely on the numerical model by Choi (1980), who has been successful in simulating major features of the tides in the Yellow Sea and the East China Sea. Specifing the boundary condition in this way, it should be remembered that the model by Choi (1980, Table. 1) produced the M2 amplitude around the Jeju-Do larger than the observed amplitudes. Therefore we know a priori that our model will also produce relatively large amplitude. However, the overall overestimation should not affect the spatial structures of the phase and amplitude variation which are the main concern of our investigation.

In Fig. 9a the tidal wave first arrives at the southeastern shore of the Jeju-Do, and progresses to the west along the northern and the southern coasts separately. Before leaving the island the wave along either side of the island merges at the northwestern shore. As for the variation of the amplitude around the island it is noticed in Fig. 9b that the amplitude on the northern coast of the island is significantly smaller than that on the southern coast with the minimum of 76. 1 cm and the maximum of 94.4 cm at locations indicated in Fig. 9b. Examining the isoplethes of the amplitude, particularly those of 90 cm and 80 cm, we find that the effect of the Jeju-Do extends half the channel between the island and the southern coast of the Korean Peninsula to the north and about a distance equivalent to the size of the Jeju-Do to the south. A meridional section of the amplitude along a line indicated in Fig. 9b is very useful to look into the major spatial variation. From the northern coast of the Jeju-Do the amplitude increases rapidly towards the southern coast of the Korean Peninsula and reaches as high as 120 cm (Fig. 10) which is much larger than the maximum on the southern coast of the Jeju-Do. Then it may be natural to ask the quation:

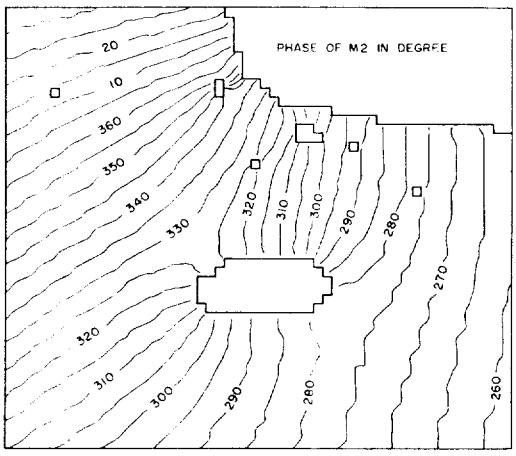

(a)

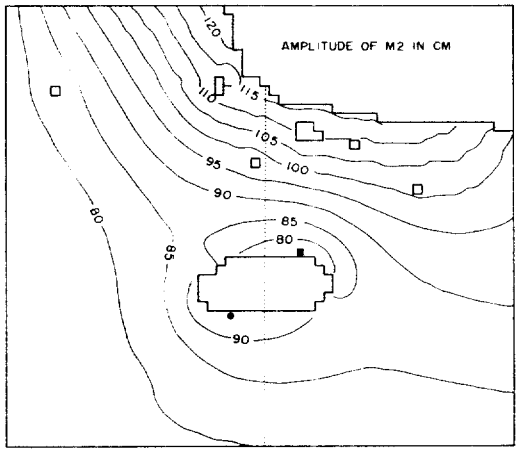

(b)

Fig. 9. Phase(a) and amplitude(b) for the M2 tide with the open boundry condition adopted from Choi (1980). In (b) closed circle (●) and square(■) indicate locations of the maximum and minimum amplitude and a section (Fig. 10) is taken along the dotted line.

why are the maxima not the same? From Eq. (2.6) we can show that the amplitude of the scattered wave takes the following nondimensional form

$$S(\xi) \propto \frac{2\omega/\sigma}{1-(2\omega/\sigma)^2}\,\frac{C}{L}$$

where L is a length scale of the primary wave such as $L = 1/\kappa$. For given ω, σ and L, the amplitude $S(\xi)$ is proportional to C that represents the size of the island. Since the southern coast of the Korean Peninsula is longer than that of the Jeju-Do, the amplitude on the former should be larger accordingly. On this regard it should be pointed out that unlike the experiment for the plane wave the open boundary conditon itself specifies larger amplitude towards the Korean coast. This boundary condition and the dynamics of wave propagation make isoplethes near the southern coast of Korean Peninsula nearly parallel to the coastline.

In theory it is well known that the scale of the trapping for an infinite coastline in a constant-depth ocean, corresponding to the rapid increase of the amplitude towards the southern coast of the Korean Peninsula, is determined by the radius of deformation, $(gh)^{1/2}/f$. If we apply this criteria in our case, the trapping distance is 340 km for $h = 75$ m. Therefore the effect of the larger amplitude on the southern coast of Korean Peninsula may extend to the south beyond the Jeju-Do which is distanced about 100 km from the Peninsula. Hence, if there were no effect of the Jeju-Do on the wave propagation, the amplitude of the M2 tide on the northern coast of the Jeju-Do would be larger than that on the southern coast of the island. In fact, we can easily interpolate isoplethes of the amplitude near the Jeju-Do from its far field in Fig. 9b. The interpolated section shown in Fig. 10 clearly indicates the gradually decaying effect of the southern coast of the Korean Peninsula. Because of this effect the difference between the amplitudes on the northern and the southern coast of the Jeju-Do is less than what it might be in the absence of the southern coast of the Korean Peninsula. If the Jeju-Do were significantly smaller than its actual size, it would scatter the wave with a much smaller amplitude and its effect could be easily buried in the large scale slope.

DISCUSSION

Performing the numerical experiment with

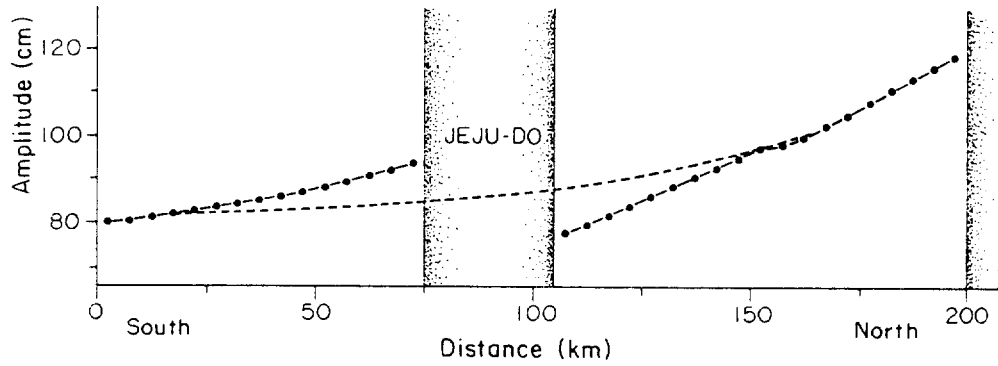

Fig. 10. Variation of the amplitude from the numerical experiment of the M2 tide along a meridional section indicated in Fig. 9. Dotted line is a sea level if there were no effect of the Jeju-Do.

all nonlinear terms in Eqs. (3. 2) and (3. 3), we obtained again the phase and amplitude of the M2 tide, almost identical with Fig. 9. The results imply that the contributon of nonlinear terms are minimal in the area of our investigation as far as the phase and amplitude distributions are concerned.

For comparison with the theory we construct two amplitude-phase diagrams; one for numerical data from the experiment of the M2 tide and the other for the observed data presented in Fig. 1. The shape of the diagram for the numerical experiment (Fig. 11) is very close to the theoretical one shown in Fig. 3. This diagram by itself is sufficient to demonstrate that the theory by Proudman (1914) is adequate to explain the scattering of the tidal wave by the Jeju-Do.

In Fig. 12 the observed phase increases in an orderly manner along the northern and southern coasts in consistence with the propagation of the tidal wave around the Jeju-Do. But the variation of the observed amplitudes does not appear to fit into an ideal amplitude-phase relationship, because of the low amplitude at the Chagui-Do (location 7 in Fig. 1). However, if we exclude this low value, the observed relationship is not far from the theoretical one. It is obvious that more data are required to resolve the shape of the relationship.

Fig 3. and 11 show that over a wide coastline the amplitude is close to its maximum and minimum. In other words the extreme amplitudes are not very sensitive to the geographical locations. Based upon this we may try a quantitative comparision utilizing available data. In Fig. 12 we notice that the amplitude at Seoguipo (location 5) and Whasun (location 6) are almost the same. Therefore we take the amplitude at Seoguipo as an estimate of the maximum. For the minimum we may choose the amplitude at Sewha (location 3), because it is smaller than the amplitudes at Whabukri (location 2) and Udo (location 4). Then the difference between the estimates of the maximum and the minimum is 16.2 cm, a little less than 18.3 cm which we obtain in the numerical experiment. However, the two differences can not be compared directly, since the amplitudes of the incident wave are not the same. The amplitude of incident wave for the numerical experiment can be estimated to be about 85 cm in Fig. 11, whereas for the real sea Fig. 12 suggests nearly 70 cm. If 70 cm were the incident amplitude for the numerical experiment, we should expect a difference of 15.1 cm. Then the observed difference of 16.2 cm and the expected difference of 15.1 cm are compared very favorably with each other.

Fig. 12 is also very useful to understand the reason why Kang (1984) reproduced the phase fairly well, but the amplitude very poorly. A

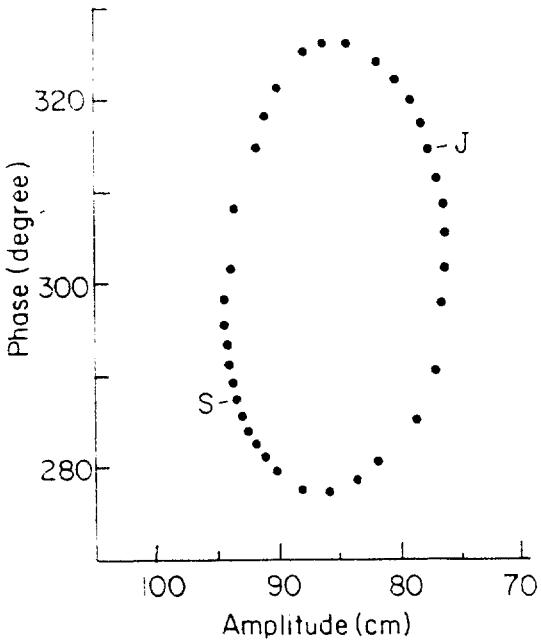

Fig. 11. Amplitude-phase diagram for the numerical experiment of M2 tide. S and J denots Seoguipo and Jeju.

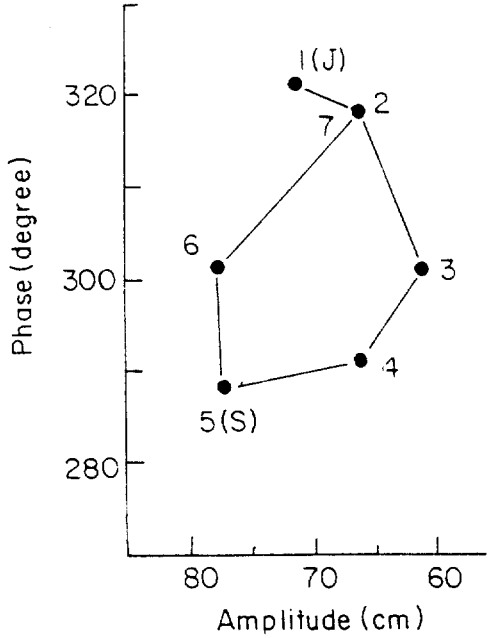

Fig. 12. Amplitude-phase diagram for the data shown in Fig. 1. S and J indicate data obtained at Seoguipo and Jeju.

clue for the poor representation of the amplitude can be found in the co-range chart producted by Kang (1984), in which locations of maximum and the minimum amplitudes of the M2 tide on the coast of the Jeju-Do are interchanged contrary to observations. Other than the misplacement of the extreme amplitudes the pattern of the amplitude variation near the Jeju-Do (Kang, 1984; Fig. 5) looks very much like Fig. 9b. It is found that a term involving the Coriolis parameter in Eq. (2.8) of Kang (1984) has a "plus" sign instead of a "minus" sign. This is equivalent physically to investigating the same problem in the southern hemisphere where the direction of angular velocity of the earth is opposite to the gravity. As the Coriolis force acts to the left of motion in the southern hemisphere, the positive and negative deviations of the amplitude appear opposite to the case of the northern hemisphere. This is the reason why Kang (1984) found the maximum and the minimum of the M2 amplitude on the northeastern and the southwestern shores of the Jeju-Do respectively. For the phase variation, it was coincident that Kang (1984) reproduced the phase with little difference between his model and the observations, because the phase variation is independent of the direction of the rotation (see Eq. (2. 2)). The observed orderly variation of the phase around the Jeju-Do also helps to minimize the difference.

CONCLUSIONS

The amplitude of the M2 tide along the southern coast of the Jeju-Do is significantly larger than that along the northern coast. To investigate this phenomena we examine the theoretical model by Proudman (1914), who considered the diffraction of a plane wave by various coastal geometries, one of which was an elliptic island. Due to the Coriolis force the amplitudes larger and smaller than the incident amplitude appear on the coast to the right and left of the wave propagation, respec-

tively, in the northern hemisphere.

Results of a numerical experiment with a plane incident wave agree very well with the theory. Another numerical experiment with open boundary conditions adopted from Choi (1980) reproduces the maximum amplitude on the southwestern coast and the minimum amplitude on the northeastern coast in consistence with observation. The pattern of the amplitude-phase diagram of these experiments is very close to that produced theoretically, indicating that the observed amplitude and phase variations of the M2 tide can be explained in terms of scattering of the wave as modeiled by Proudman (1914).

ACKNOWLEDGEMENTS

We are deeply thankful to the Hydrographic Office of Korea for providing the tidal data and to Dr. Byung Ho Choi for the results of his numerical experiment and careful reading of the manuscript. Prof. Jong Yul Chung supported part of our numerical experiments generously. This research started in 1980 during our field experiment around the Jeju-Do supported by the Korean Science and Engineering Foundation.

REFERENCES

Choi, B.H. 1980. A tidal model of the Yellow Sea and the East China Sea. Korea Ocean Research and Development Institute Rep., KORDI-80-02, pp. 72.

Flather, R.A and N.S. Heaps. 1975. Tidal computations for Morecambe Bay. Geophysical J. Roy. Astron. Soc., **42**: 489-517.

Hydrographic Office. 1982. Marine enviromental atlas of Korean Water. Pub. No. 1451, pp. 41.

Kang, Y.Q. 1984. An analytic model of the M2 tide near Cheju Island. J. Oceanol. Soc. Korea, **19**: 18-23.

Ogura, S. 1933. The tides in the seas adjacent to Japan. Bull. Hydrogr. Depart. Imper. Japanese Navy, **7**: 1-189.

Pedlosky, J. 1979. Geophysical Fluid Dynamics. Springer-Verlag, New York. pp 624.

Proudman, J. 1914. Diffraction of tidal waves on flat rotating sheet of water. Proc. Lond. Math. Soc., 2nd ser., **14**: 89-102.

Received August 11, 1986
Accepted August 23, 1986